Remote Sensing of Mountain Birch Forest Biomass and Leaf Area Index Using ASTER Data

J. Heiskanen

Department of Geography, University of Helsinki, P.O. Box 64, FIN-00014 Helsinki, Finland – janne.heiskanen@helsinki.fi

Abstract – Suitability of ASTER satellite data for estimating biomass and LAI for mountain birch forests was investigated. The field data consisted of 124 plots surveyed in northernmost Finland in July 2004. The statistical relationships between the field measurements and ASTER reflectances were modelled using canonical correlation analysis (CCA) and reduced major axis (RMA) regression. The models were applied to map biomass and LAI, and to calculate biomass and LAI statistics for most widespread subalpine mountain birch forest types in the study area. The results indicate significant relationships between biomass, LAI and ASTER data. The estimates were reasonable when compared to the previously published data and to the biotope inventory data. The predictions seem to be unreliable when dwarf birch shrubs are abundant in the undergrowth. However, ASTER VNIR bands in particular seem to have potential for vegetation mapping.

Keywords: ASTER, biomass, canonical correlation analysis, leaf area index, mountain birch forest, regression analysis

1. INTRODUCTION

Birch forests are dominant over extensive areas north of the boreal coniferous forest belt in northern Fennoscandia (Hämet-Ahti, 1963). Mountain birch (*Betula pubescens* ssp. *czerepanovii*) is the most common tree or scrub in the area forming the treeline both to the north and at high elevations. The mountain birch forests are subject to natural and human induced changes, which emphasise the need for mapping the current state and monitoring the dynamics of these ecosystems. Mountain birch ecosystems are important in the global carbon budget and likely to be affected by increasing temperatures, atmospheric CO^2 content and prolongation of the growing season. The mountain birch forests are also affected by the grazing and trampling of semi-domestic reindeer and defoliated regularly by insect herbivores.

Biomass and leaf area index (LAI) are important variables in many ecological and environmental applications, for example, in the regional ecosystem models (e.g. Nemani *et al.*, 1993). Accurate estimation of biomass is required for carbon stock accounting and monitoring. LAI is defined as one half of the total leaf area per unit ground surface area, and it controls many biological and physical processes in the water, nutrient and carbon cycle.

There are only a few studies concerning the biomass and LAI of the mountain birch forests. However, the biomass proportioning of single mountain birch trees have been examined and allometric equations developed to approximate the biomass of single trees according to, for example, diameter at breast height (DBH) or height (e.g. Starr *et al.*, 1998; Dahlberg *et al.*, 2004). The allometric relationships have also been employed to give plot-wise biomass and LAI estimates, but the laborious field work has limited the studies to single plots or to a small number of plots.

The possibility to estimate biomass and LAI by remote sensing has been investigated in a number of studies at various spatial scales and environments (e.g. Nemani *et al.*, 1993). Remote sensing has shown potential to extrapolate the limited amount of field data to give regional estimates of biomass and LAI. Furthermore, remote sensing can provide the biomass and LAI surfaces that can be analysed in the geographical information systems (GIS) and input to the ecological models. However, only a very few studies have attempted to estimate biomass and LAI for mountain birch forests using remote sensing (Heiskanen, submitted).

In this study, the suitability of the Advanced Spaceborne Thermal Emission and Reflection Radiometer (ASTER) data for estimating biomass and LAI for mountain birch forests was investigated. The statistical relationships between the forest parameters and ASTER reflectances were modelled. The models were applied to map biomass and LAI, and to calculate biomass and LAI statistics for three widespread subalpine mountain birch forest types. The results were compared to the published biomass and LAI values, and to the stand-wise biotope inventory data.

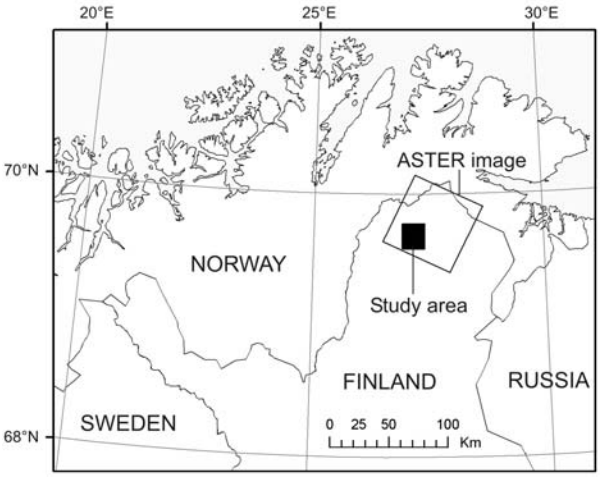

Figure 1. Location of the study area.

* Field work was financed by Finnish Cultural Foundation.

2. MATERIAL AND METHODS

2.1 Study area

The study area is located in Utsjoki, in northernmost Finland (Fig. 1). The area lies north of the continuous pine forest and it is characterised by the subalpine mountain birch forests, gently sloping low fells, and mires. The study area is situated in the orohemiarctic zone at the northern boundary of the northern boreal zone. The most widespread mountain birch forest types are subalpine *Empetrum-Lichenes* type (sELiT), subalpine *Empetrum-Lichenes-Pleurozium* type (sELiPlT) and subalpine *Empetrum-Myrtillus* type (sEMT) (Hämet-Ahti 1963). The forest types differ in terms of soil moisture, canopy cover and species composition of the undergrowth vegetation.

2.2 Field data

The field data consisted of 124 plots surveyed in July 2004. The field data was collected from four 1×1 km^2 sites located in the different forest types with variable tree densities and shrub covers. The plots were located by GPS. The surveyed data consisted of the basic stand parameters for trees taller than 1.3 m, the plot size being either 100 m^2 or 200 m^2 depending on the tree density. The aboveground tree biomass (t ha^{-1}) (hence called biomass) was estimated using the measured DBH and the allometric models developed by Starr *et al.* (1998). LAI (m^2 m^{-2}) was calculated using the estimated leaf biomass and specific leaf weight values (SLW) published by Kause *et al.* (1999). The other reference data included the biotope inventory data covering the most of the study area. The inventory data included the biotope type, and canopy closure (%) and stand volume (m^3 ha^{-1}) estimates. The inventory is based on the visual interpretation of the aerial photographs.

2.3 Satellite data

The satellite data consisted of the atmospherically corrected surface reflectance product of ASTER scene recorded on 29 July 2000. ASTER has three spectral bands in the visible to near-infrared (VNIR) and six bands in the shortwave infrared (SWIR) spectral regions (Table A). The ASTER data was rectified to the national coordinate system using ground control points (GCPs) and first order polynomials. The GCPs were collected from digital topographic maps in 1:20 000 scale. The total RMSE was 0.65 pixels (9.75 m) for VNIR bands and 0.58 pixels (17.4 m) for SWIR bands. The topographic effects were reduced using the C-factor method (Teillet *et al.*, 1982) and DEM in 25 m cell size.

2.4 Data analysis

Reflectances were calculated for the field plots by taking an average reflectance inside 25 metre buffer zones. The averaging was made in order to reduce the geometric errors in the GPS measurements and rectification, and to remove the difference in the pixel size between the VNIR and SWIR bands. The relationships between biomass, LAI and ASTER data were examined in detail by Heiskanen (submitted). The method employed in this study corresponds closely to the linear multiple regression analysis, and it was proposed by Cohen *et al.* (2003). The multispectral image was converted into a single band index using the canonical correlation analysis (CCA). The canonical weights were computed separately for biomass and LAI. The stepwise regression analysis was applied to select only the significant bands before CCA ($p < 0.05$). The relationship between biomass, LAI and CCA scores was modelled using the reduced major axis (RMA) regression. Two-thirds of the data (83 cases) was employed in the modelling and one-third (41 cases) was used for testing. The plot-level estimation errors were studied by RMSE and bias statistics.

Table A. Specifications of ASTER bands.

Subsystem	Band	Spectral range (μm)	Spatial resolution (m)
VNIR	1	0.52–0.60	15
	2	0.63–0.69	
	3	0.76–0.86	
SWIR	4	1.600–1.700	30
	5	2.145–2.185	
	6	2.185–2.225	
	7	2.235–2.285	
	8	2.295–2.365	
	9	2.360–2.430	

2.5 Biomass and LAI mapping

The developed regression models were applied to map biomass and LAI over the study area. The whole ASTER image was converted into CCA scores using the previously determined weights. The SWIR band was resampled to a 15 m resolution to match the pixel size of the VNIR data. The unsupervised Isodata classification was applied to mask water and pine forests. A mire mask was derived from the biotope inventory data. The descriptive statistics were calculated for the different mountain birch forest types using the biotope polygons. Finally, the statistics were compared to the biomass and LAI values in the literature, and biomass and LAI estimates to the stand volume and canopy cover data of the biotope inventory.

3. RESULTS AND DISCUSSION

There is a significant relationship between biomass and LAI of the mountain birch forests, and ASTER reflectances. The red band 2 has the strongest correlation against biomass ($r = -0.831$) and LAI ($r = -0.847$). Bands 1, 2, 3 and 9 were the only significant ($p < 0.05$) explanatory variables in the stepwise regression analysis, and were used in CCA. Log-transformed bands 1, 2 and 9 were used because the transformation enhanced the linear correlation. Band 9 was the only SWIR band employed, which suggest that ASTER SWIR data has only little explanatory power in the biomass and LAI modelling in the mountain birch forests. The derived CCA scores explained 84% and 85% of the variability in biomass and LAI, respectively. RMSE was 3.45 t ha^{-1} (40.97%) for biomass and 0.28 m^2 m^{-2} (36.96%) for LAI estimates. Biases, -0.60 t ha^{-1} (-7.16%) and -0.11 m^2 m^{-2} (-14.86%), were not significant ($p > 0.05$).

Fig. 2 shows the predicted biomass and LAI maps. The patterns are very similar because of the high correlation between the two parameters (r = -0.985). Table B shows the means and standard deviations of the biomass and LAI values calculated using the biotope inventory data. The statistics were calculated for all the polygons that had biomass or LAI over 0, i.e. were covered by trees. Table B also shows the biomass and LAI values for subalpine heath and forest vegetation reported in the literature. Although all the values are not directly comparable, the estimates seem to be reasonable in comparison to the results of the previous studies.

Medians, interquartile ranges, and extreme values are summarised for biomass and LAI in Fig. 3. Similar statistics were also derived for stand volume and canopy cover from the biotope inventory data. The most luxurious sEMT type has considerably higher biomass and LAI values than the two drier types. Range of the values is the largest in the most widespread sELiPlT type. The distributions of the biomass and LAI values are similar to those of stand volume and canopy cover.

Furthermore, the biomass and LAI estimates are plotted against stand volume and canopy cover in Fig. 4. There is a significant relationship between biomass and stand volume, and between LAI and canopy cover. However, the correlation is weak if stands with relatively high shrub cover are considered. The most common shrubs in the mountain birch forests are dwarf birch (*Betula nana*) and juniper (*Juniperus communsis*). Dwarf birch has very similar reflectance to mountain birch, although the height of the shrub is typically only from 0.2 to 0.8 m. Biomass and LAI seem to be overestimated in the stands where shrubs are particularly abundant. Therefore, only the polygons having shrub cover less than 20% were used for calculating the statistics in the Table B and Fig. 3. Fig. 4 shows also that the biomass and LAI values begin to saturate slightly in the highest stand volumes and canopy covers.

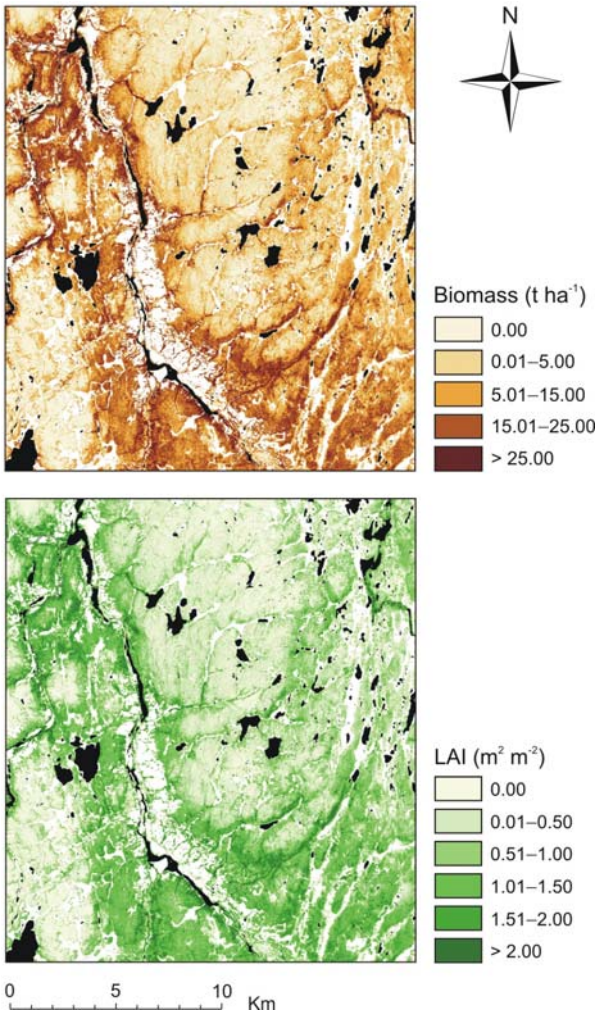

Figure 2. Predicted biomass and LAI surfaces. Waters are in black, and pine forests and mires in white.

Table B. Biomass and LAI values reported in the literature in comparison to this study.

Study	Vegetation / mountain birch forest type	Biomass (t ha^{-1})[a]	LAI (m^2 m^{-2})
Kjelvik & Kärenlampi, 1975	Birch forest	8.53	-
	Low alpine heath, birch bush	1.92	-
Kjelvik & Kärenlampi, 1975	Subalpine birch forest	23.90	-
Starr *et al.*, 1998	Subalpine *Empetrum-Myrtillus* type (sEMt)	21.20	-
Bylund and Nordell, 2001	*Empetrum* type, lichen-dominated variant	9.57	1.44
Dahlberg *et al.*, 2004	Wind-exposed heath	1.09	0.09
	Snow-protected heath and meadow	7.65	0.52
	Birch forest	27.49	2.06
This study	Subalpine *Empetrum-Lichenes* type (sELiT)	4.71 (3.85)[b]	0.44 (0.31)
	Subalpine *Empetrum-Lichenes-Pleurozium* type (sELiPlT)	9.24 (5.85)	0.78 (0.46)
	Subalpine *Empetrum-Myrtillus* type (sEMt)	19.05 (5.02)	1.55 (0.38)

[a] total aboveground tree biomass
[b] mean (standard deviation)

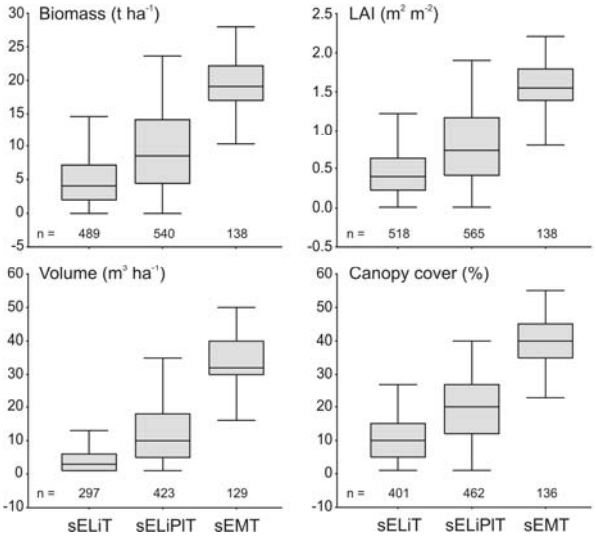

Figure 3. Summaries of the biomass, LAI, stand volume and canopy cover for the studied mountain birch forest types.

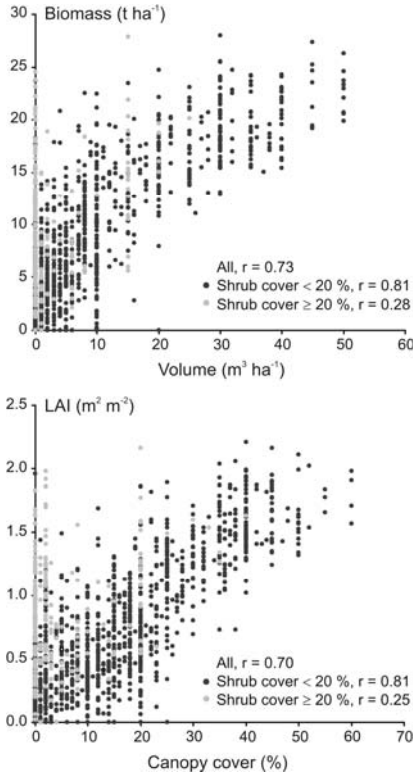

Figure 4. Biomass and LAI plotted against stand volume and canopy cover.

4. CONCLUSIONS

This study demonstrates the potential of optical satellite data, e.g. ASTER data, to map biomass and LAI in the mountain birch forests using a relatively small amount of field data. The results were reasonable when compared to the literature and to the biotope inventory data. However, in comparison to the previously published biomass and LAI values, the values reported here are based on a relatively large number of forest stands. The stands having high abundance of dwarf birch shrubs in the undergrowth were excluded from the statistics because predictions were considered unreliable. ASTER data has not been used extensively in the study of vegetation due to the limited data availability. However, the good spatial resolution of the VNIR bands and the availability of the higher order data products make ASTER an interesting data source for vegetation mapping.

ACKNOWLEDGEMENTS

The author thanks NASA, METI, ERSDAC and LP DAAC for providing the ASTER data, and Metsähallitus for providing the biotope inventory data.

REFERENCES

Bylund, H. & Nordell, K.O. (2001). Biomass proportion, production and leaf nitrogen distribution in a polycormic mountain birch stand (*Betula pubencens ssp. czerepanovii*) in northern Sweden. In F.E. Wielgolaski (Ed.), *Nordic mountain birch ecosystems*, pp. 115–126.

Cohen, W.B., Maiersperger, T.K., Gower, S.T. & Turner, D.P. (2003). An improved strategy for regression of biophysical variables and Landsat ETM+ data. *Remote Sens. Environ.* 84: 561–571.

Dahlberg, U., Berge T.W., Peterson, H. & Vencatasawmy, C.P. (2004). Modelling biomass and leaf area index in a sub-arctic Scandinavian mountain area. *Scand. J For. Res.* 19: 60–71.

Heiskanen, J. (submitted). Estimating aboveground tree biomass and leaf-area index (LAI) in a mountain birch forest using ASTER satellite data.

Hämet-Ahti, L. (1963). Zonation of the mountain birch forests in northernmost Fennoscandia. *Ann. Bot. Soc. 'Vanamo'* 34: 1–127.

Kause, A., Haukioja, E. & Hanhimäki, S. (1999). Phenotypic plasticity in foraging behavior of sawfly larvae. *Ecology* 80: 1230–1241.

Kjelvik, S. & Kärenlampi, L. (1975). Plant biomass and primary production of Fennoscandian subarctic and subalpine forests and alpine willow and heath ecosystems. In F.E. Wielgolaski (Ed.), *Fennoscandian tundra ecosystems. Part 1: Plants and microorganisms*, pp. 111–120.

Nemani, R., Pierce, L., Running, S. & Band, L. (1993). Forest ecosystem processes at the watershed scale: sensitivity to remotely-sensed leaf area index estimates. *Int. J. Remote Sensing* 14: 2519–2534.

Starr, M., Hartman, M. & Kinnunen, T. (1998). Biomass functions for mountain birch in the Vuoskojärvi Integrated Monitoring area. *Boreal Env. Res.* 3: 297–303.

Teillet, P.M., Guindon, B. & Goodenough, D.G. (1982). On the slope-aspect correction of multispectral scanner data. *Can. J. Remote Sensing* 8: 84–106.